MIJST
MIST International Journal of Science and Technology

Effect of Non-Uniform Soiling on Solar Panel Output and Revenue Analyzed Through a Controlled Experiment by Using a Designed I-V Scanner

Mohammad Didarul Islam[1], Md. Aminul Islam[2], and M. Ryyan Khan[3*]

[1,2]Department of Electrical, Electronic and Communication Engineering, Military Institute of Science and Technology (MIST), Dhaka, Bangladesh
[3]Department of Electrical and Electronic Engineering, East West University (EWU), Dhaka, Bangladesh

emails: *[1]didarulislam357@gmail.com; [2]aminul@eece.mist.ac.bd; and [3]ryyan@ewubd.edu*

ARTICLE INFO

Article History:

Received: 20th March 2022
Revised: 29th June 2022
Accepted: 10th August 2022
Published: 29th December 2022

Keywords:

PV panel
I-V characteristics curve
I-V scanner
bottom edge soiling
non-uniform soiling
performance loss factor
PV power plants

ABSTRACT

Non-uniform soiling drastically decreases the power generation of PV panels. Different events are responsible for the non-uniform soiling on PV panels for example bird droppings, sand storms, or snowfall. In this study, we have achieved multiple-goals for analyzing the effect of non-uniform soiling on a PV module output. We also analyzed the revenue losses due to the non-uniform soiling in a PV power plant. Firstly, for observing the effect of non-uniform soiling an I-V scanner has been designed. Secondly, the designed I-V scanner has been used to observe the changes in the I-V characteristics curve of PV panels due to non-uniform soiling and shading conditions. In this study, we have conducted various controlled experiments by providing different shading conditions on the PV panel and observing the I-V curve changes. A correlation has been done with the various shadowing conditions like the bottom edge soiling condition of PV panels or bird-dropping. In a PV power plant, non-uniform soiling may occur at the edge of PV panels after cleaning intervention. Considering these scenarios, we have done an economic analysis for determining the effect of non-uniform soiling on the revenue of PV power plants. Finally, the relations between the cleaning cycle, performance loss factor, and solar cell area coverage with respect to revenue have been also discussed in this article.

1. INTRODUCTION

When sunlight reaches the glass surface of a solar panel, it passes through the cells that generates electricity. Even if a solar panel is in great condition, its power production will be lowered if sunlight is blocked by any means, such as bird droppings or unevenly accumulated soiling.

Non-uniform soiling on the surface of PV modules affects the I-V characteristics curve of the PV panel and causes hotspots. The temperature of the hotspot is definitely connected to non-uniform soiling, soil band structure, and non-uniform soiling (Lorenzo *et al.*, 2014; Qasem *et al.*, 2014; Sulaiman *et al.*, 2011). As a result, the performance of PV modules varies depending on a variety of conditions, as seen by variations in the I-V characteristics curve. As a result, a transportable I-V scanner can be an important tool for assessing non-uniform shading on solar panels in the field (Pereira *et al.*, 2021).The soil might collect unevenly on the bottom edge of the panels after manual or robotic cleaning. The PV panel's power output will be reduced if the bottom solar cell of any string is covered by non-uniformly collected dirt. The non-uniform soiling effect on a PV module has been shown in previous research to be greater than uniform soiling (Maghami *et al.*, 2016; Molin, 2018; Schill *et al.*, 2015). Soiling accumulates more towards the bottom and, in rare events, at the top of the PV module. Wind and water from dew or rain have a role in this buildup (Lorenzo *et al.*, 2014; Qasem *et al.*, 2014). The collection of dust at the bottom corners of PV modules can cause a significant loss in performance (Pigueiras *et al.*, 2014). The bottom edges of PV modules with lower tilt degrees are more prone to soiling buildup (Gostein *et al.*, 2013; Molin, 2018). The cleaning water flow is frequently insufficient to move these dust particles, resulting in a constant buildup of dust in various forms near the bottom edges of the PV module. The PV module is often installed in portrait or landscape orientation (Cui *et al.*, 2021; Karthick *et al.*, 2020). Rectangular, triangular, and

transverse trapezoidal forms of accumulated soiling band morphologies have been detected at the bottom edge of the PV module (Cui *et al.*, 2021). Partially shading and soiling bands generated at the bottom edges of the PV module restrict incoming sunlight penetration into the solar cells, resulting in a hotspot (AlDowsari *et al.*, 2014). The collection of soiling and bird droppings, which is strongly associated with the soiling accumulating region (Kazmerski *et al.*, 2017), can also cause this localized overheating hotspot of the PV module. Moreover, during the field research, the entire region covered by non-uniformly distributed deposited soiling and bird droppings revealed a high temperature (Cui *et al.*, 2021). These panel hotspots may cause irreversible damage to the PV system. Compared to the non-soiling region, the fixed area covered by accumulated soiling may store some water after cleaning or raining for a long period on the module surface, which can weaken the PV module seal and reduce the PV panel's service life (Cui *et al.*, 2021). Solar farms are planned with row-to-row shadowing panels in mind. Non-uniform shading caused by residual soiling at numerous edges and irregular bird droppings can significantly reduce farm productivity; nevertheless, these factors are not considered in farm designs (Gökdağ *et al.*, 2018; Manganiello *et al.*, 2015). In the PV module, a bypass diode is utilized to reduce the mismatching of the coupled solar cells. Generally, the bypass diode is connected in parallel with a **15** to **20** solar cell series connection to reduce the mismatching due to shadings. PV modules in shade have been the subject of much research since they change the IV shapes (Gallardo-Saavedra & Karlsson, 2018). The majority of economic research analysis in the past has been done with uniform soiling accumulation in consideration. According to an economic study conducted in the Middle East and Africa, the best cleaning cycles for a PV power plant are 5 to 6 days, with a normalized income of **97.5** percent and a loss of **2.5** percent. It shows, that the optimum cleaning cycle in North America is more than 21 days, with revenue losses ranging from **2**% to **5**%. The optimum cleaning cycle in the European region is 17 days, with a revenue loss of more than **2**% (Mithhu et al., 2021). We developed a portable and simple I-V scanner for observing changes in the I-V properties of a PV module under operational conditions in this research. Because all of the components for this I-V scanner is readily accessible on the local market, it will be highly handy, inexpensive, and effective for use in research and rapid system assessment. The goal of this proposed study is to see how partial or non-uniform shade on PV panels owing to soiling on the bottom edge of the modules or random bird droppings affects their performance.

The impact of partial or non-uniform shadowing on various solar cells is investigated in this controlled experiment. Solar cells are chosen at random and covered in various percentages of their surface area to see how shade affects solar panel I-V and power. The relationship between PV module generated power and shade covering the area in (%) is discussed, with soiling and bird-dropping conditions associated. Although this type of partial shade differs from the more well-known row-to-row shading, it should be carefully handled to avoid sub-optimal solar farm operations. However, there seems to be an insufficient study on the relationship between partial shade caused by non-uniformly deposited soiling and bird dropping and PV module power generation efficiency. PV generating output is severely reduced by non-uniform soiling. It has a significant impact on diminishing the income of PV power plants in a PV power plant. Due to the non-uniform soiling of PV panels, even if the cleaning procedure is performed on a regular schedule, power generation may not increase.

In this study, we have done different selective controlled experiments. After the experiments, the evaluation of the economic analysis considering the effect of non-uniform soiling in the different cleaning cycles was also done. The economic analysis of the decreasing factor of the PV panel performance ratio is also addressed at the end of this study.

2. EXPERIMENTAL SETUP

A. *Development* of I-V scanner

We used an n-channel MOSFET (IRF540) as a non-linear variable load in the I-V scanner design. The basic idea is that the I-V curve of the MOSFET will alter depending on the gate-to-source voltage (VGS). The panel now has an electrically adjustable, variable load. The MOSFET's I-V curve will intersect with the PV module's I-V curve at various operating points. As a result, the I-V characteristics curve of the PV module may be captured by measuring a collection of crossing points of MOSFET and PV module I-V curves. When the gate to source voltage (VGS) is increased, When the MOSFET is operated as a non-linear load for the PV panel, the MOSFET's I-V characteristics curve overlaps the PV module's I-V characteristics at particular operating points, as shown in Figure 1, the module I-V characteristics can then be formed automatically by reading these intersecting or operational points.

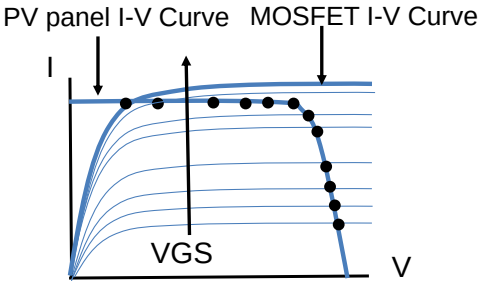

Figure 1: Intersection regions in MOSFET and PV module I-V characteristics curves

B. *Connection of PV Modules*

In our experiment, we used 30 W PV modules from Solarland (model number: SLP030-12). Each PV module is made up of 36 solar cells that are joined in two strings in series. T30-watt PV modules are linked in series to conduct the experiment. Each module has two bypass diodes, helping to make our panel arrangement a four-bypass-diode system. Two PV modules are wired in series in which is shown in Figure 2(a). The system has four strings of solar cells, as shown in Figure 2(b). Partial shadings or non-uniform soiling events such as bird droppings, sand storms, or snowfall events are mitigated with a bypass diode on each string.

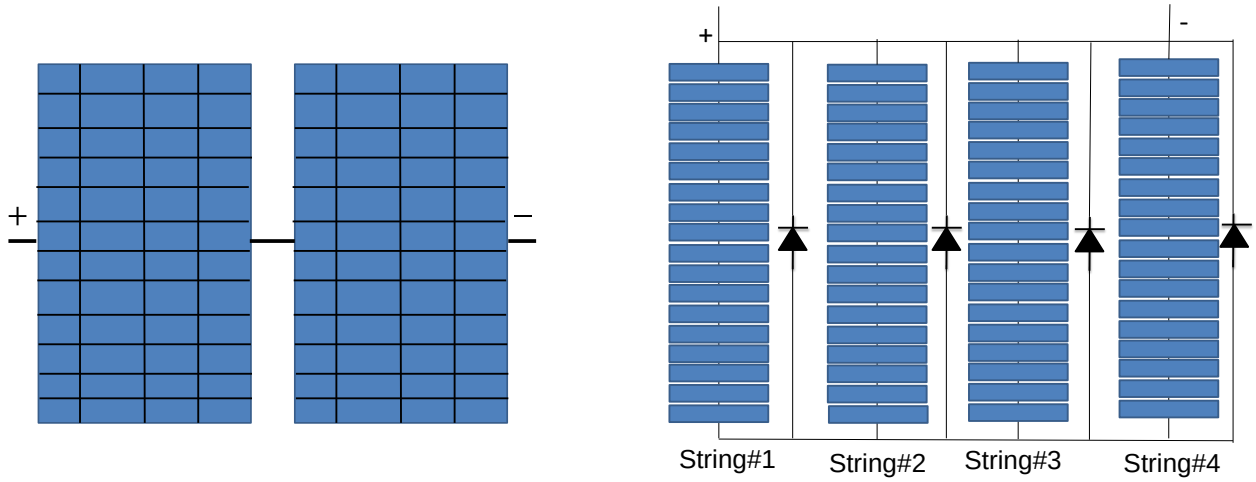

(a) (b)

Figure 2: PV modules, (a) connection, (b) string and bypass diode connections

Table 1
Electrical Parameters of a PV Module

Items	Symbols	Values
Maximum power	P_{max}	30 Watt
Operating voltage	V_{mp}	17.2 Volt
Operating current	I_{mp}	1.74 Ampere
Open circuit voltage	V_{OC}	21.6 Volt
Short circuit current	I_{SC}	1.93 Ampere

C. Schematic Diagram of I-V Scanner

The circuit schematic of the developed I-V scanner is shown in Figure 3. A triangle wave of $5V$ peak is supplied to the MOSFET gate terminal from the triangular wave generator to switch the MOSFET IRF540. The triangle control signal ensures that the panels' I-V are scanned continuously and automatically. The peak voltage of the triangle wave is $5V$, and its period is $2s$. The drain terminal of the MOSFET is linked to the PV module's positive $(+)$ terminal. Between the PV module terminals, a voltage divider with an 8:1 division ratio is utilized. $R2 = 2k$ and $R1 = 16k$ are chosen to ensure this ratio. The main objective of this voltage divider is to keep the data logger input to the Arduino Mega's analog port below 5 volts. Because the series-connected PV module's open-circuit voltage is nearly $40\,V$, using $8{:}1$ voltage divider ratio reduces the PV module's voltage reading to $5\,V$. The center of the divider resistors R1 and R2 is used to measure the voltage of the PV module (V). The obtained value is properly rescaled during the measurement of PV module voltage (V) (multiplied by 9). The MOSFET's source terminal is wired to the grounds through the 1Ω ceramic resistor, which reads the PV module's current (I) through another analog pin on the data logger. To read each operational point, the current (I) and voltage (V) measurements are monitored sequentially.

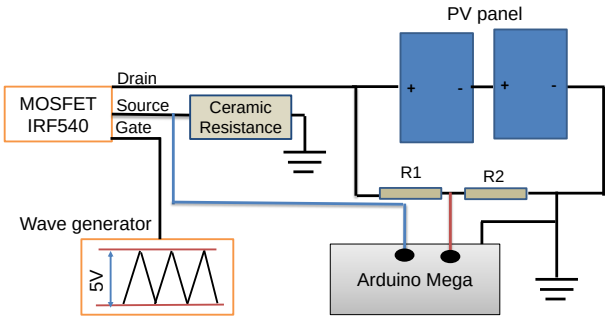

Figure 3: I-V scanner schematic circuit diagram

3. EXPERIMENT RESULTS AND INTERPRETATION

We selectively cover portions of the solar cells in the panel's arrangement to analyze partial shade conditions and measure the I-V and energy outputs. PV module 2 was uncovered, but individual solar cells within PV module 1 were successively covered (partially shaded) in order to study changes in the PV panel setup's I-V characteristics curve. Table II summarizes the results of the trials that were carried out (labeled A, B, C, and D). The solar cell area covers (percent) utilized in the experiment is shown in Figure 4(a). On a cell, a percentage of the area was covered (with black cello tape): 0% (no shade), 25%, 50%, 75%, or 100%. Figure 4(b) depicts experiment B, in which one solar cell is chosen at random (from PV module 1, string 1) to be tested for changes in the I-V curve at 0%, 25%, 50%, 75%, and 100% area-cover circumstances. Experiment C is represented in Figure 4(c), in which one solar cell (from PV module 1, string 1) was randomly covered 25%, 50%, 75%, and 100% and then another random cell (from module 1, string 2) was arbitrarily covered from 25% to 100%. Figure 4(d) depicts experiment D, in which one solar cell is covered to a depth of 25% and another is covered to a depth of 100% both solar cells are inside the same string in experiment D (*i.e.*, in PV module string 1). The experiment of the I-V scanner and a practical illustration of expC2 are described in Table 2. Figure 4(e) and 4(f) represent the experimental setup example which is stated in Table 2.

Table 2
Description of the Conducted Experiments

Experiments	Category	% covered
Experiment A (String1)	expA1	one cell 25% covered
	expA2	another cell 25% covered
Experiment B (String1, One PV Cell selectively)	expB1	Not covered
	expB2	25% covered
	expB3	50% covered
	expB4	75% covered
	expB5	100% covered
Experiment C (String 1, randomly one cell 25% fixed cover, String 2 one cell selectively)	expC1	25% covered
	expC2	50% covered
	expC3	75% covered
	expC4	100% covered
Experiment D (String 1, randomly one cell 25% fixed cover, and another PV cell of string1)	expD1	25% cover
	expD2	50% cover
	expD3	75% cover
	expD4	100% cover

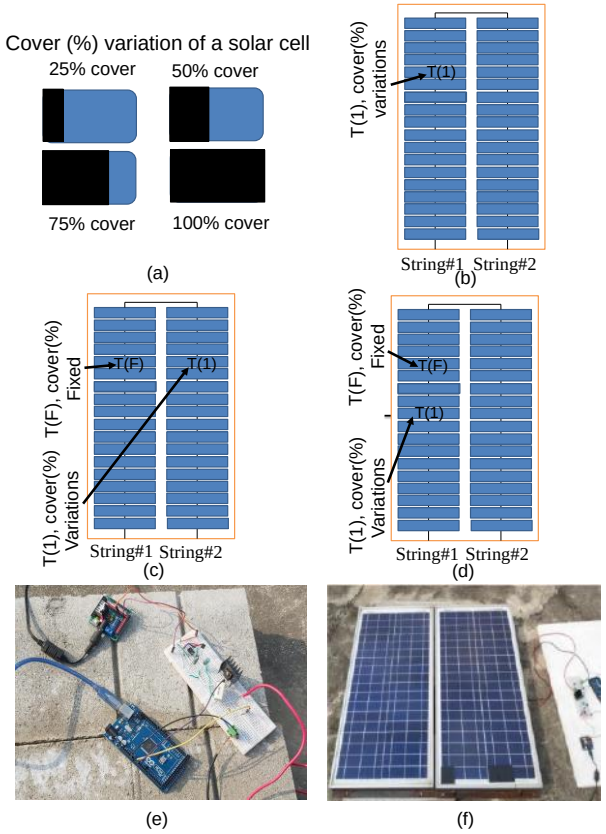

Figure 4: (a) The variance in each solar cell cover (percentage) has been defined. The following are examples of different experiment conditions: (b) experiment B: string 1 solar cell cover (percent) variations, (c) experiment C: string1 fixed **25**% cover, string 2 individual cell cover (percent) variations, (d) experiment D: string1 fixed **25**% cover, string1 another cell cover (percent) variations (e) I-V scanner setup for testing. (f) An example of a conducted experiment, such as table-II's expC2

We controlled shade conditions that were similar to realistic non-uniform shading scenarios (sandstorms, snowfall, bird droppings) during the experiment. The level of non-uniformity in different soiling scenarios are unpredictable. To eliminate this uncertainty, we conducted a controlled experiment in which the area of a certain solar cell was shaded at various percentages. With the use of black cello tape covering, we demonstrated what would happen if non-uniform soiling shaded the panel in various percentages of its area. The variations in power output caused by non-uniform soiling will be similar to those seen in our controlled experiment.

A. Normalized Data Analysis

During the infield experiments, we observed that the irradiance of sunlight varies from one I-V measurement to the next. This made it difficult to compare the I-V characteristics from the various experiments. Therefore, we have introduced the normalization technique, where, the current and voltage readings of an I-V are normalized to its corresponding short circuit current and open circuit voltage. All the I-V curves in Figure 5 discussed in the following have been normalized.

The normalized I-V curves from experiment A are shown in Figure 5(a). The I-V characteristics are overlapping in this case. Similarly, the P-V curves of two trials, expA1 and expA2, overlap in Figure 5(b). The overlapping curves in Figure 5(a) and 5(b) illustrate that, regardless of the position of the cell, we should expect the same relative output reduction because of the same shadow coverage. To retain have same short circuit current, the bypass diode is activated at lower voltages. The I-V characteristics are overlapping in this case. Similarly, the P-V curves of two trials, expA1 and expA2, overlap in Figure 5(b). The normalized I-V curve of experiment B is shown in Figure 5(c), where each solar cell in string1 has a 25%, 50%, 75%, and 100% cover. The overlapping curves in Figure 5(a) and 5(b) illustrate that, regardless of the position of the cell, we should expect the same relative output reduction because of the same shadow coverage. We found the maximum power production under a 0% cover situation as shown in Figure 5(d). The normalized output power for the PV cell shading area covered ranging from 25% to 100% is shown in Figure 5(d). When the coverage is increased from 0% to 25% to 50%, the maximum power (Pmax) is seen to decrease. Because the bypass diode is activated at the maximum power point, the Pmax measurement does not change for 50% to 100% shading.

The I-V curve characteristics for all of the examples of experiment C are shown in Figure 5(e) (string 1 solar cell fixed 25% cover, and another cell coverage varied from 25% to 50%, 75%, and 100%). As a result, string 1 bypass activated at 25% current in all scenarios. It appears that the coverage of the same amount of area of two strings in exp-C1 (25% + 25% coverage) has the same impact as in exp-B with 25% shadow. The string 2 bypass diode activated again for 50 percent, 75 percent, and 100 percent coverage of the solar cell of string 2 in exp-C2, exp-C3, and exp-C4, respectively. Because string 1 is likewise 25% shaded, the bypass diode triggered MPP will have a 25% lower Pmax, as seen in Figure 5(f). The I-V

and P-V characteristics of experiment D are depicted in Figure 5(g) and 5(h). One cell in this experiment is shaded 25%, while shading on another PV cell in the same string is changed. The impact of shading in two cells is dominated by the increased shadow coverage due to the fact that they are both under the same bypass diode. As a result, experiment D exhibits the same patterns as experiment B.

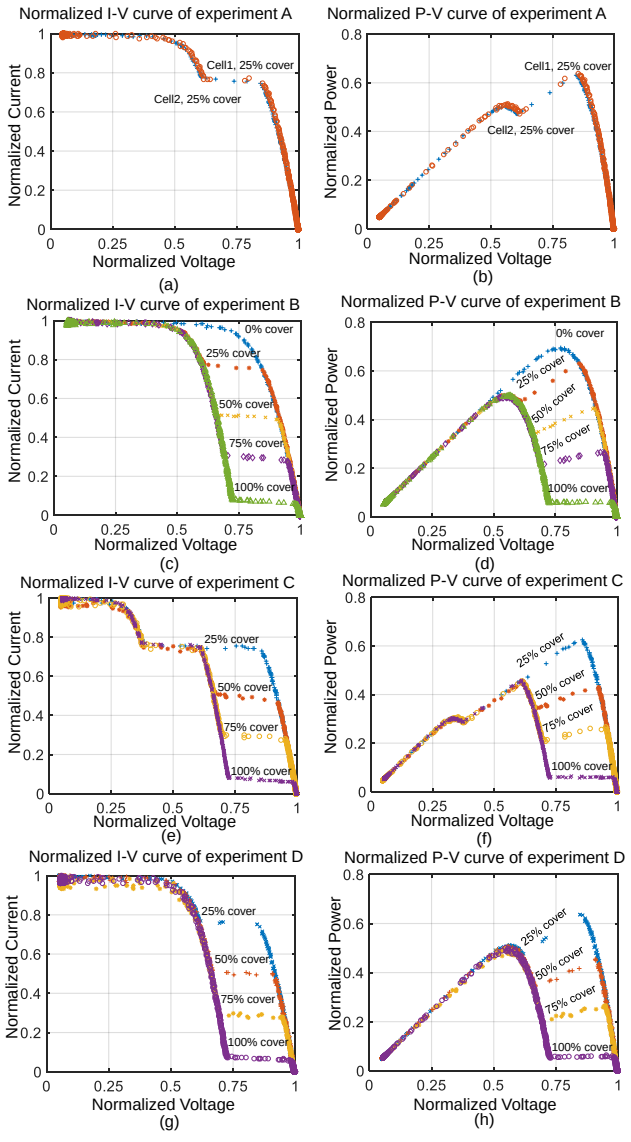

Figure 5: (a) I-V curve of experiment A (a cell of string 1, **25**% cover; another cell of string 1, **25**% cover), (b) P-V curve of experiment A, (c) I-V curve of experiment B (string 1 cell **0**%, **25**%, **50**%, **75**%, and **100**% cover variation), (d) P-V curve of experiment B, (e) I-V curve of experiment C (string 1, a cell with a **25**% fixed cover, string 2 another randomly selected cell, **0**%, **25**%, **50**%, **75**%, and **100**% cover variation), (f) P-V curve of experiment C, (g) I-V curve of experiment D (string 1, a cell with a **25**% fixed cover, string 1 another randomly selected cell, **0**%, **25**%, **50**%, **75**%, and **100**% cover variation), (h) P-V curve of experiment D

B. Experiment B, C, and D MPP Comparison

The maximum power ($P_{\max}$) of studies B, C, and D are compared in Figure 6. Solar cell area coverage changes as follows for experiment B: 0%, 25%, 50%, 75%, and 100% from PV module1 string 1. The PV panel's power is at its greatest when there is no covering. We found that the power decreased monotonically as the proportion of shadowing on the solar cell increased up to 50%.

$P_{\max}$ remains unchanged for cell shading of 50% or more. This is because, in high-shading conditions, the shaded string is discarded due to the bypass diode activation. The MPP peak changes to a lower voltage owing to the activation of bypass diodes, as seen in Figure 5 (P-V plots).

Because of shading on a single string, experiments B and D are nearly identical, as discussed in the preceding subsection.

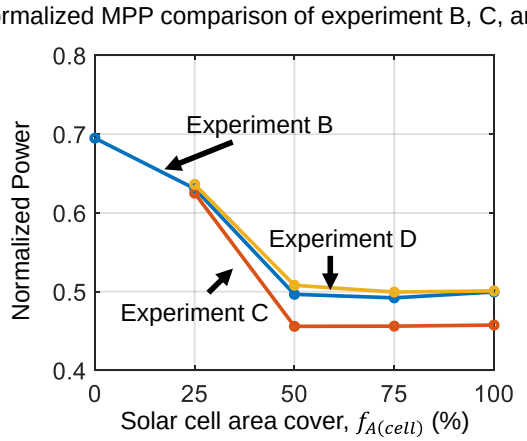

Figure 6: Maximum power ($\boldsymbol{P_{max}}$) comparison of experiments B, C, and D

However, we can observe that its $P_{\max}$ saturates at a lower value (for shading 50%) in the figure for experiment C. After the MPP is limited by the bypass diode in this scenario (i.e., exp-C), the current at the second string is also reduced by 25% shading. As a result, the normalized power for the shade of 50% or more in experiment C is lower than in experiments B or D.

C. Multiple Soiling Band Condition

There are three types of soiling bands along the bottom border of a solar panel, according to the literature: triangular, rectangular, and transverse trapezoid. The triangular soiling band shape seen in Figure 7(a) mostly covers a cell from string 1 and partially covers a cell from string 2.

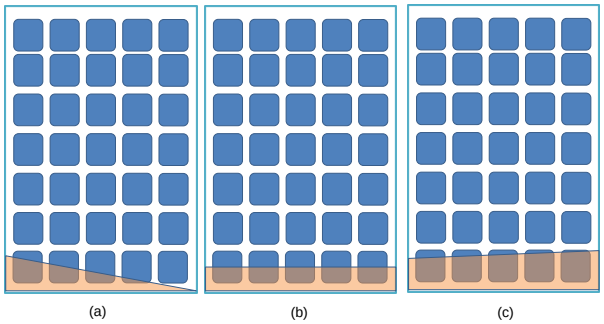

Figure 7: Soiling band schematic diagram (a) triangular, (b) rectangular, (c) transverse trapezoidal schematic diagram on PV panel.

The rectangular soiling band form is shown in Figure 7(b) covers the bottom border of both cells of the two strings. A transverse trapezoidal soiling band is seen in Figure 7(c). Even after cleaning, such soiling bands can linger on panels, especially if machine-cleaning is utilized. All three options are applicable to our experiment C. As previously stated, even partial shading of a few cells can drastically reduce the system's output, therefore the success of cleaning should be regularly reevaluated if such soiling bands remain.

Bird-dropping has the potential to shade various cells on the panel at random (Sisodia & Mathur, 2019). The bird-dropping in PV panels in distinct strings in different regions of a PV panel. All of our experimental results can be linked to the effects of low to high bird dropping rates on panel output. A cumulative soiling and bird-dropping scenario significantly reduce production; the appropriate operational output will then be lost unless a thorough cleaning intervention is performed.

4. REVENUE ANALYSIS FOR NON-UNIFORM SOILING

In case of uniform soiling on modules, the performance ratio, PR (unclean to clean panel output ratio) decreases daily due to dust accumulation. After a cleaning intervention, PR immediately resets to unity. The temporal characteristics of PR is saw-tooth-like with periodic cleaning-this is shown in Figure 8(a). Clearly, PR is not always equal to 1, this indicates unavoidable energy loss for any cleaning cycle t_C (> 1). The cleaning cycle and its costs are chosen to maximize revenue. The revenue under uniform soiling with a cleaning cycle of t_C can be written as shown in Equation (1).

$$\text{Rev}_\text{U} = RE_0\left[1 - \frac{1}{2}at_C - \frac{C}{RE_0}\frac{1}{t_C}\right] \quad (1)$$

Here, R is the tariff rate, a is the soiling rate, E_0 is the mean daily rated (*i.e.*, clean panel) energy output, C is the cleaning cost, and t_C is the cleaning cycle.

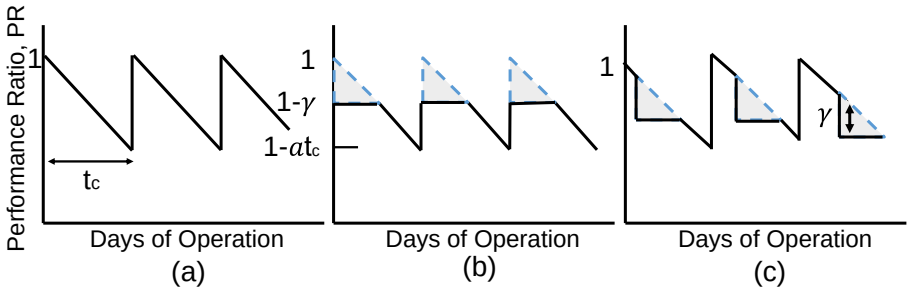

Figure 8: Performance ratio versus cleaning cycle (a) without non-uniform soiling, (b) with non-uniform soiling conditions (edge soiling due to machine or manual cleaning), and (c) with non-uniform soiling conditions (bird-droppings, snowfall, sand storm)

Consider a scenario where there is always some accumulated dust (*e.g.*, as shown in Figure 7(b)) at the edges. In this case, after inefficient machine cleaning, the PR does not return to unity, see Figure 8(b). We define this residual loss through the "Performance Loss (PL) Factor", γ. With time, the module will continuously accumulate uniform dust with no reduction in PR until the rest of the module area reaches soiling-loss comparable to that at the edges. Therefore, after each inefficient cleaning cycle, the PR reaches $(1-\gamma)$. The additional loss per cycle is marked are the shaded triangular area. The corresponding mean daily loss in PR related to this triangular area is $(\gamma^2/2a)$. A similar loss may occur due to a sudden soiling band formation due to wind, or bird dropping (see Figure 8(c)).

For the uniform soiling, the PR can decrease by $\sim at_C$ at the end of a cleaning cycle. Therefore, if $\gamma > at_C$, the uniform soiling on the panel area never reaches the edge-soiling loss of γ. In such a case, the performance ratio always remains at $PR = \gamma$ showing no effect or signature of cleaning. Finally, the revenue under combined uniform and non-uniform soiling with the cleaning cycle of t_C can be written as:

$$\text{Rev}_\text{NU} = \begin{cases} RE_0\left[1 - \frac{1}{2}at_C - \frac{C}{RE_0}\frac{1}{t_C} - \frac{\gamma^2}{2a}\right]; & \gamma < at_C \\ RE_0\left(1 - \gamma - \frac{C}{RE_0}\frac{1}{t_C}\right) & ;\gamma \geq at_C \end{cases} \quad (2)$$

The term (C/RE_0t_C) accounts for the loss in revenue due to panel cleaning at each cleaning cycle.

Finally, the performance loss factor γ can be related to the solar cell area cover fraction ($f_{A(cell)}$) from Figure 6. The fractional loss in 'Normalized power' with increasing $f_{A(cell)}$ is equivalent to γ. Therefore, a second-order polynomial fit gives:

$$f_{A(cell)} = -5\gamma^2 + 3.2\gamma \quad (3)$$

Equations (2) and (3) relate the revenue (Rev_NU) to the solar cell area cover fraction ($f_{A(cell)}$) due to non-uniform soiling in presence of constant uniform soiling (rate: a).

Figure 9 and 10 show the normalized revenue and the revenue is the presence of uniform non-uniform soiling. Normalized revenue is the dust-affected revenue normalized to the soiling-free revenue of a solar farm. The revenue, of course, considers the reduction in cash-inflow due to costs incurred by periodic panel cleaning. In our calculations, we assume values relevant to South Asia: $R = 0.0895$ USD/kWh , $E_0 = 0.1123$ kWh/day , $C = 0.03$ USD/kWh/Wp , $a = 0.8\%/day$ (Jahangir *et al.*, 2020; Mithhu *et al.*, 2021).

With, $f_{A(cell)} = 0$ (i.e., $\gamma = 0$), there is no non-uniform soiling. However, as shown in Figure 9, due to natural

uniform soil accumulation the normalized revenue f_R is 97%, 94%, and 88% for cleaning cycles of $t_C = 7$, 15, and 30 days, respectively. This means we will lose 3%, 6%, and 12% of the rated clean-panel revenue during these cleaning cycles, it is impossible to reduce the revenue loss to zero in presence of soiling. The corresponding revenue values are shown in Figure 10. With increased non-uniform soiling (*e.g.*, due to inefficient cleaning), $f_{A(cell)} > 0$ and the revenue decreases further (as explained in Equation (2)).

The non-uniform soiling, i.e., $f_{A(cell)} > 0$ can have a strong reduction in revenue. Interestingly, for $f_{A(cell)} > 25\%$ cleaning cycles of 7 and 15 days result in similarly reduced revenues, the loss is $> 10\%$. This extraordinarily high loss will persist unless the panels and their edges are appropriately cleaned. In the unlikely case when $f_{A(cell)} > 45\%$, $t_C = 7$, 15, or 30 days result in the same $> 20\%$ loss in revenue.

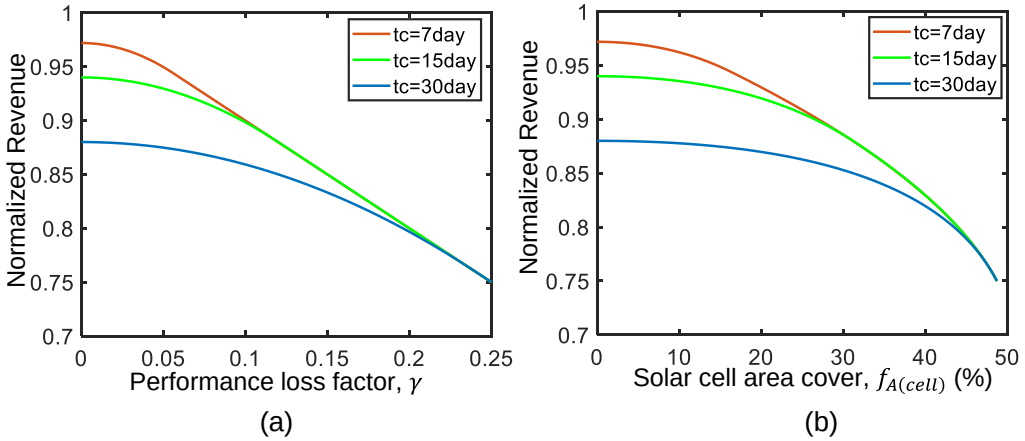

Figure 9: Relationship between (a) normalized revenue and decreasing factor of performance ratio (γ) (b) normalized revenue and covered area (%) due to non-uniform soiling

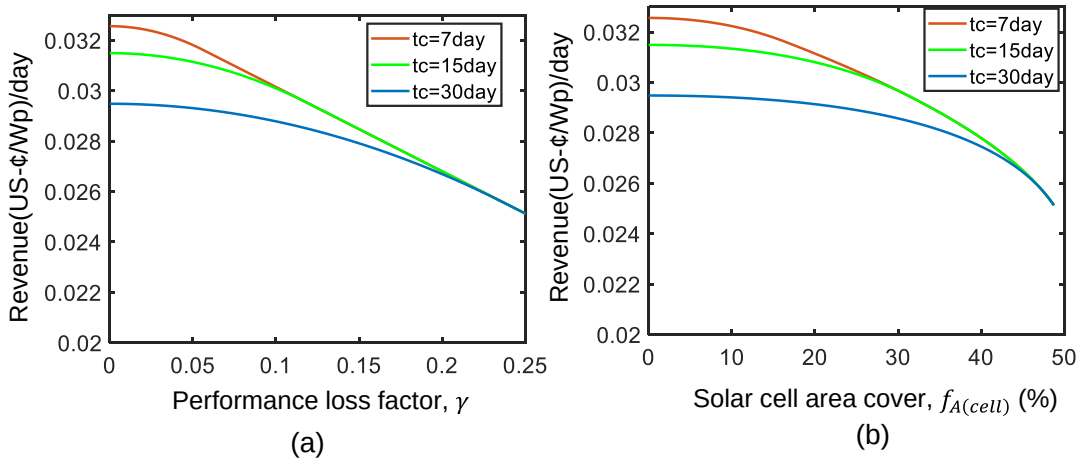

Figure 10: Relationship between (a) revenue and decreasing factor of performance ratio (γ) (b) normalized revenue and covered area (%) due to non-uniform soiling.

5. CONCLUSION

In this work, we have designed an I-V scanner for observing the I-V changes. Various experiment has been done by providing various shadowing conditions. These shading conditions correlated with different real-life scenarios like bird-dropping. After that, we modelled a numerical analysis for evaluating economic analysis where the non-uniform soiling conditions are considered. The relationship of revenue between performance loss factor and area cover (%) due to non-uniform soiling is also shown in this study.

During the experiment, we have found the I-V characteristics curve of a PV panel changes abruptly with respect to the different shadowing conditions. In a string of a PV panel when around 50% shadow occurred then the bypass diode of that string is triggered therefore then the output power does not change even if the area coverage increases. We have found that the cleaning cycle has a significant influence on the non-uniform soiling effect. In non-uniform soiling conditions for 7 days cleaning cycle, the normalized revenue becomes 97%, and for the cleaning cycle of 15 and 30 days, the revenue becomes 94% and 88% respectively. Surprisingly for cleaning cycles 7 and 15 days, if the area of non-uniform soiling on a solar cell is greater than 25% then the decrease of revenue for both cleaning cycle become the same. Therefore, in these rated cleaning cycles it is impossible to avoid the effect of non-uniform soiling on the PV panels. From the study, we found the lower the cleaning cycle the lower the loss due to non-uniform soiling. Non-uniform soiling on PV panels can reduce the power generation of a PV panel drastically. The effect of non-uniform soiling cannot be mitigated until the

cleaning intervention is performed. To ensure maximum revenue, engineers designing PV power plants should take into account the condition of non-uniform soiling in PV panels on different cleaning cycles.

ACKNOWLEDGEMENTS

Authors would like to express their gratitude to the department of EECE, MIST, Dhaka, Bangladesh; and department of EEE, EWU, Dhaka, Bangladesh. They are also grateful to the Editors and Reviewers of MIJST for valuable suggestions and comments in improving the contents of the article.

REFERENCES

AlDowsari, A., Bkayrat, R., AlZain, H., & Shahin, T. (2014). Best practices for mitigating soiling risk on PV power plants. *2014 Saudi Arabia Smart Grid Conference (SASG)*, 1–6. https://doi.org/10.1109/SASG.2014.7274291

Cui, Y.-Q., Xiao, J.-H., Xiang, J.-L., & Sun, J.-H. (2021). Characterization of Soiling Bands on the Bottom Edges of PV Modules. *Frontiers in Energy Research*, *9*, 145. https://doi.org/10.3389/fenrg.2021.665411

Gallardo-Saavedra, S., & Karlsson, B. (2018). Simulation, validation and analysis of shading effects on a PV system. *Solar Energy*, *170*, 828–839. https://doi.org/10.1016/j.solener.2018.06.035

Gökdağ, M., Akbaba, M., & Gulbudak, O. (2018). Switched-capacitor converter for PV modules under partial shading and mismatch conditions. *Solar Energy*, *170*, 723–731. https://doi.org/10.1016/j.solener.2018.06.010

Gostein, M., Littmann, B., Caron, J., & Dunn, L. (2013). *Comparing PV power plant soiling measurements extracted from PV module irradiance and power measurements*. 3004–3009. https://doi.org/10.1109/PVSC.2013.6745094

Jahangir, J. B., Al-Mahmud, Md., Sarker Shakir, Md. S., Hasan Mithhu, Md. M., Rima, T. A., Sajjad, R. N., & Khan, M. R. (2020). Prediction of Yield, Soiling Loss, and Cleaning Cycle: A Case Study in South Asian Highly Construction-Active Urban Zone. *2020 47th IEEE Photovoltaic Specialists Conference (PVSC)*, 1371–1374. https://doi.org/10.1109/PVSC45281.2020.9300606

Karthick, A., Manokar Athikesavan, M., Pasupathi, M. K., Manoj Kumar, N., Chopra, S. S., & Ghosh, A. (2020). Investigation of Inorganic Phase Change Material for a Semi-Transparent Photovoltaic (STPV) Module. *Energies*, *13*(14), 3582. https://doi.org/10.3390/en13143582

Kazmerski, L. L., Diniz, A. S. A. C., Braga, D. S., Maia, C. B., Viana, M. M., Costa, S. C., Brito, P. P., Campos, C. D., de Morais Hanriot, S., & de Oliveira Cruz, L. R. (2017). Interrelationships Among Non-Uniform Soiling Distributions and PV Module Performance Parameters, Climate Conditions, and Soiling Particle and Module Surface Properties. *2017 IEEE 44th Photovoltaic Specialist Conference (PVSC)*, 2307–2311. https://doi.org/10.1109/PVSC.2017.8366584

Lorenzo, E., Moretón, R., & Luque, I. (2014). Dust effects on PV array performance: In-field observations with non-uniform patterns: Dust effects on PV array performance. *Progress in Photovoltaics: Research and Applications*, *22*(6), 666–670. https://doi.org/10.1002/pip.2348

Maghami, M. R., Hizam, H., Gomes, C., Radzi, M. A., Rezadad, M. I., & Hajighorbani, S. (2016). Power loss due to soiling on solar panel: A review. *Renewable and Sustainable Energy Reviews*, *59*, 1307–1316. https://doi.org/10.1016/j.rser.2016.01.044

Manganiello, P., Balato, M., & Vitelli, M. (2015). A Survey on Mismatching and Aging of PV Modules: The Closed Loop. *IEEE Transactions on Industrial Electronics*, *62*(11), 7276–7286. https://doi.org/10.1109/TIE.2015.2418731

Mithhu, Md. M. H., Rima, T. A., & Khan, M. R. (2021). Global analysis of optimal cleaning cycle and profit of soiling affected solar panels. *Applied Energy*, *285*, 116436. https://doi.org/10.1016/j.apenergy.2021.116436

Molin, M. D. (2018). Experimental Analysis of the Impact of Soiling on Photovoltaic Modules Performance. *Master's Thesis. Milan: Politecnico Di Milano*.

Pereira, T. A., Schmitz, L., dos Santos, W. M., Martins, D. C., & Coelho, R. F. (2021). Design of a Portable Photovoltaic I–V Curve Tracer Based on the DC–DC Converter Method. *IEEE Journal of Photovoltaics*, *11*(2), 552–560. https://doi.org/10.1109/JPHOTOV.2021.3049903

Pigueiras, E., Moretón, R., & Luque, I. (2014). Dust effects on PV array performance: In-field observations with non-uniform patterns. *Progress in Photovoltaics: Research and Applications*, *22*. https://doi.org/10.1002/pip.2348

Qasem, H., Betts, T., Müllejans, H., Albusairi, H., & Gottschalg, R. (2014). *Dust-induced shading on photovoltaic modules*. https://doi.org/10.1002/PIP.2230

Schill, C., Brachmann, S., & Koehl, M. (2015). Impact of soiling on IV-curves and efficiency of PV-modules. *Solar Energy*, *112*, 259–262. https://doi.org/10.1016/j.solener.2014.12.003

Sisodia, A., & Mathur, R. (2019). Impact of bird dropping deposition on solar photovoltaic module performance: A systematic study in Western Rajasthan. *Environmental Science and Pollution Research*, *26*. https://doi.org/10.1007/s11356-019-06100-2

Sulaiman, S. A., Hussain, H. H., Leh, N. S. H. N., & Razali, M. S. I. (2011). Effects of Dust on the Performance of PV Panels. *International Journal of Mechanical and Mechatronics Engineering*, *5*(10), 2021–2026. https://publications.waset.org/10305/effects-of-dust-on-the-performance-of-pv-panels